Rescue of Glaucoma-Causing Mutant Myocilin Thermal Stability by Chemical Chaperones

J. Nicole Burns[†,§], Susan D. Orwig[†,§], Julia L. Harris[†], J. Derrick Watkins[†], Douglas Vollrath[‡], and Raquel L. Lieberman*[,†]

[†]School of Chemistry and Biochemistry, Georgia Institute of Technology, 901 Atlantic Drive NW, Atlanta, Georgia 30332 and [‡]Departments of Genetics and Ophthalmology, Stanford University School of Medicine, 300 Pasteur Drive, Stanford, California 94305. [§]These authors contributed equally to this work.

Open angle glaucoma (OAG) is a recent addition to the family of protein conformational disorders. OAG is a heterogeneous disease characterized by irreversible vision loss often associated with elevations in intraocular pressure (1, 2). The mechanisms that lead to intraocular pressure increases are poorly understood but are thought to occur in the anterior region of the eye within the anatomical pathway for outflow of aqueous humor, which includes the trabecular meshwork extracellular matrix (TEM) (3, 4). In the last 10 years, causative genes that account for inherited, autosomal-dominant glaucoma cases have been identified, of which mutations in myocilin are by far the most common (1). Myocilin (gi accession: 4557779, geneID 4653), a secreted glycoprotein (3), is proposed to play a structural role in the TEM and to limit the migration of human trabecular meshwork (HTM) cells (5). Myocilin contains a signal sequence, a linker with a putative N-glycosylation site, a coiled-coil/leucine zipper for multimerization and interactions with certain extracellular matrix proteins (6–8), and a ~30 kDa olfactomedin (OLF) domain in which the majority of genetic lesions leading to OAG are located. More generally, emerging roles of OLF domains include involvement in adhesion and neuronal growth as well as in development of the mammalian brain (9). The prevalence and sequence conservation (~60–80% identity among mammals) of OLF domains among eukaryotes underscores the need for structural and functional studies.

Recent evidence supports a toxic gain-of-function disease mechanism for mutant myocilin. Instead of secretion to the TEM, mutant myocilins have been shown to accumulate in the endoplasmic reticulum (ER) of HTM cells with toxic consequences (10, 11). In cell-based assays, growth at lower temperatures enables the secre-

ABSTRACT Mutations in myocilin cause an inherited form of open angle glaucoma, a prevalent neurodegenerative disorder associated with increased intraocular pressure. Myocilin forms part of the trabecular meshwork extracellular matrix presumed to regulate intraocular pressure. Missense mutations, clustered in the olfactomedin (OLF) domain of myocilin, render the protein prone to aggregation in the endoplasmic reticulum of trabecular meshwork cells, causing cell dysfunction and death. Cellular studies have demonstrated temperature-sensitive secretion of myocilin mutants, but difficulties in expression and purification have precluded biophysical characterization of wild-type (wt) myocilin and disease-causing mutants *in vitro*. We have overcome these limitations by purifying wt and select glaucoma-causing mutant (D380A, I477N, I477S, K423E) forms of the OLF domain (228–504) fused to a maltose binding protein (MBP) from *E. coli*. Monomeric fusion proteins can be isolated in solution. To determine the relative stability of wt and mutant OLF domains, we developed a fluorescence thermal stability assay without removal of MBP and provide the first direct evidence that mutated OLF is folded but less thermally stable than wt. We tested the ability of seven chemical chaperones to stabilize mutant myocilin. Only sarcosine and trimethylamine N-oxide were capable of shifting the melting temperature of all mutants tested to near that of wt OLF. Our work lays the foundation for the identification of tailored small molecules capable of stabilizing mutant myocilin and promoting secretion to the extracellular matrix, to better control intraocular pressure and to ultimately delay the onset of myocilin glaucoma.

*Corresponding author,
raquel.lieberman@chemistry.gatech.edu.

tion of mutant myocilins, suggesting that when protein production is slowed, toxicity is reduced (*11–13*). The myocilin variants secreted at permissive temperatures likely retain a native-like three-dimensional structure but have compromised stability due to a local perturbation caused by the mutation. Importantly, mice heterozygous and homozygous for a myocilin knockout allele (*14*) and human individuals with N-terminal myocilin mutations (*15*) do not exhibit ocular abnormalities.

Proteins like mutant myocilins that are folded in the ER are prevented from cellular trafficking if they are not folded correctly. ER quality control proteins recognize features/flaws in a newly folded protein. A misfolded protein is then either refolded to its native state or targeted for degradation. Even minor defects in structure remote from a functional site of the protein cannot escape the highly redundant ER quality control system that can detect exposed hydrophobic patches in soluble proteins and mobile loops and in generally reduced compactness, *i.e.*, biophysical properties (*16*). ER quality control does not test newly folded proteins for function, which may be preserved for a missense mutant that retains a native-like structure.

Ineffective clearing of mutant myocilins leads to aggregation, cell stress, and eventually death (*10, 12, 17–19*). HTM cell dysfunction death is thought to lead to a compromised TEM unable to properly control eye pressure and, eventually, to the retinal degeneration characteristic of glaucoma. Thus, the pathophysiology is not linked directly to abolished intrinsic function, but first to a defect in myocilin stability, then to a defect in cellular trafficking, ER stress, and finally to reduced function of the TEM.

Mechanisms that stabilize a mutant protein in its native state or accelerate the rate of folding and enable it to meet ER quality control standards hold promise as therapy for protein-misfolding diseases (*20*). The ability to traffic mutant protein with residual function out of the ER is hypothesized to reduce toxicity and cell stress, allowing for partial restoration of function, which will ultimately delay the onset of clinical symptoms (*21*). In the case of mutant proteins without a known ligand or molecular structure, such as myocilin, screening for tailored small molecules that accomplish these goals requires a top-down approach, *i.e.*, without knowledge of specific surface binding patches.

Although one of the major challenges to studying molecular properties of myocilin has been the difficulty in recombinant expression of a soluble, well-behaved species, we have overcome this limitation. We developed a new high-yield expression and purification system for the C-terminal region of myocilin (MYOC-OLF) comprising the OLF domain and representative glaucoma-causing mutants. We also developed a facile fluorescence thermal stability assay and used this system to gain insight into the biophysical characteristics of wt and mutant myocilins and to identify chemical chaperones that thermally stabilize the mutant proteins. Taken together, our results set the stage for studies to further evaluate the nature of the aggregated myocilin species as well as to identify therapeutic compounds that both exert a specific stabilizing effect on myocilin and enhance mutant myocilin secretion in cells.

RESULTS AND DISCUSSION

Expression and Purification of Wild-Type MYOC-OLF. We focused on the myocilin OLF domain because this is the location of 90% of all known glaucoma-causing mutations (http://www.myocilin.com/variants.php). MYOC-OLF is a monomer, harbors no predicted glycosylation sites, and has a single disulfide bond (*22, 23*).

A major challenge to the study of myocilin is its propensity to aggregate. Myocilin inclusions have been observed for both overexpressed wt myocilin in *D. melanogaster* eyes (*19*) as well as mutant myocilin in cell culture (*17*), suggesting that myocilin aggregation may be relevant to both sporadic and inherited forms of glaucoma. Poor yield and solubility is common among previous reports of *in vitro* expression of myocilin, and/or OLF domain in a soluble form using a variety of heterologous hosts (*6, 23, 24*), or refolded from *E. coli* inclusion bodies (*25, 26*). Experiments conducted on recombinant myocilin and/or OLF have been limited to concentrations of 0.05–0.1 mg mL^{-1}, with aggregation observed at higher concentrations (*6*).

We generated a soluble OLF construct that can be produced at high yield (~2 mg purified protein L^{-1} culture), purified to homogeneity, and concentrated to at least 10 mg mL^{-1} (Figure 1, panel a) by fusion to maltose binding protein (MBP) *via* an eight amino acid linker. MBP is known to facilitate proper folding of difficult proteins in *E. coli* (*27*). The short linker proved superior to the long linker fusion constructs we tested in which the purified protein coeluted with the *E. coli* folding chaperone GroEL. Expression levels of MBP-OLF were increased, and GroEL was eliminated, with the use of a

BURNS *ET AL.*

codon-correcting *E. coli* strain, rich media, and growth after induction at 18 °C.

Cytosolic wild-type MBP-OLF (MBP-OLF(wt)), purified first by amylose affinity chromatography, is a mixture of aggregated, monomeric MBP-OLF and MBP likely from cleavage by cellular proteases. Fractionation by size-exclusion chromatography (SEC) reveals these species. A ~72 kDa MBP-OLF monomer is isolated (Figure 1, panel b) in which the OLF disulfide bond remains intact (Supplementary Table S1). A second, void volume, peak corresponds to a cytosolic aggregated species. The intensity of this peak compared to that of the monomer is not sensitive to incubation at 4 °C (Supplementary Figure S1), freeze−thaw, or concentration loaded on the column. Reducing sodium-dodecyl-sulfate polyacrylamide gel electrophoresis (SDS-PAGE, Supplemental Figure S1a(inset)) reveals that the aggregates are identical to monomeric MBP−OLF, but the species do not interconvert (Supplementary Figure S1, panels a and b). The relationship of this cytosolic *E. coli* aggregate species to inclusions observed in cellular glaucoma studies (*19, 28*) is unknown but could be further evaluated in the context of improper disulfide bond formation as well as the observed high β-sheet content for OLF (*23*) and its predicted amyloid propensity (*29*).

As a consequence of the short link, accessibility of Factor Xa to the cleavage site is compromised. Cleavage for monomeric MBP-OLF(wt) is only observed at
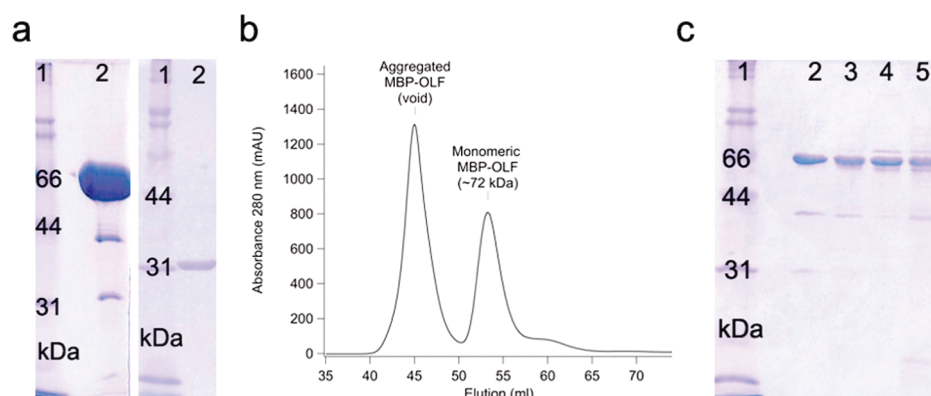

Figure 1. Protein purification. a) SDS-PAGE analysis of purified MBP-OLF(wt) and cleaved MYOC-OLF. Left: lane 2, purified, concentrated (monomeric) MBP-OLF(wt) (72 kDa, ~10 mg mL⁻¹). Right: lane 2, cleaved MYOC−OLF (~31 kDa, ~0.5 mg mL⁻¹). b) SEC chromatograph of MBP-OLF(wt) displaying aggregated MBP-OLF and monomeric MBP-OLF. c) SDS-PAGE analysis of purified MBP-OLF mutants. Lane 2, MBP-OLF (D380A); lane 3, MBP-OLF (I477S); lane 4, MBP-OLF (I477N); and lane 5, MBP-OLF (K423E). Low levels of MBP (~40 kDa) do not impede thermal stability measurements (see text). Gels include molecular mass standards as lane 1.

37 °C. Cleaved MYOC-OLF (~31 kDa) can be isolated from uncleaved MBP-OLF and from MBP upon further purification (Figure 1, panel a). No precipitation is observed for MYOC-OLF concentrated to over 5 mg mL⁻¹, nor appreciable aggregation or degradation is observed by SEC or SDS-PAGE, even after prolonged incubation at 4 °C (Supplementary Figure S1).

Expression and Purification of Mutant MBP-OLFs. The four mutant myocilins selected for this study are well documented in terms of prevalence among glaucoma patients and aggregation behavior in cells. They represent mild (D380A) (*30*), moderate (I477S) (*31*), and severe phenotypes (I477N (*32*), K423E (*33*)) as well as changes in size, polarity, and charge. The locations of these mutations within the OLF structure are not known.

TABLE 1. Summary of solubilization and secretion behaviors reported for select mutant myocilins of relevance to the current study[a]

Mutation	Glaucoma phenotype	*In vitro* solubilization (*56*)	Secretion from 37 °C culture HEK293 (*12*)/ HTM (*13*)	Secretion from 30 °C culture HEK293 (*12*)/ HTM (*13*)	ER retention (*10, 19*)
D380A	Mild	+	±	+/+	n.d.
I477S	Moderate	−	−/n.d.	+/n.d.	n.d.
I477N	Severe	−	−/−	±	+
K423E	Severe	−	−/−	−/−	+

[a](+) Positive measurement for solubilization, secretion, or ER retention, as indicated by column heading; (−) negative measurement for respective measurements; and (n.d.) measurement not determined.

TABLE 2. Effects of osmolytes on proteins investigated in this study

	Protein only	+Betaine	ΔT_m	+Glycerol	ΔT_m	+4-PBA[a]	ΔT_m	+Proline	ΔT_m	+Sarcosine	ΔT_m	+Sucrose	ΔT_m	+TMAO	ΔT_m
MBP-OLF	52.7 ± 0.8	59.6 ± 0.8	6.9	56.0 ± 1.2	3.3	55.5 ± 0.5	2.8	57.2 ± 0.3	4.5	65.2 ± 0.6	12.5	64.3 ± 0.1	10.6	64.1 ± 0.7	11.4
MBP-OLF(D380A)	46.7 ± 0.5	50.8 ± 0.2	4.1	49.5 ± 0.2	2.8	47.2 ± 0.1	0.5	49.9 ± 0.2	3.2	58.3 ± 0.6	11.6	54.2 ± 0.7	7.5	55.6 ± 0.9	8.9
MBP-OLF(I477S)	41.9 ± 0.5	48.0 ± 0.6	6.1	45.1 ± 0.2	3.1	42.6 ± 0.1	0.7	45.3 ± 0.3	3.4	54.0 ± 0.4	12.0	50.7 ± 0.2	8.7	52.7 ± 0.8	10.7
MBP-OLF(I477N)	40.1 ± 0.8	45.1 ± 0.7	4.9	43.7 ± 0.4	3.5	41.4 ± 0.4	1.3	43.8 ± 0.9	3.7	52.5 ± 0.3	12.4	50.3 ± 0.9	10.2	50.1 ± 0.8	9.9
MBP-OLF(K423E)	40.5 ± 0.1	45.9 ± 0.6	5.4	42.6 ± 0.2	2.0	38.9 ± 0.4	−1.6	42.7 ± 0.7	2.1	48.6 ± 0.6	8.1	46.3 ± 0.5	5.7	48.8 ± 0.7[a]	8.3
MBP	67.1 ± 0.3	71.3 ± 0.6	4.2	68.2 ± 0.4	1.1	66.2 ± 0.1	−0.9	69.8 ± 0.6	2.7	75.1 ± 1.0	8.0	72.6 ± 0.8	5.5	74.4 ± 0.1	7.3

[a]5 mM 4-PBA. [b]5 M TMAO.

In cellular studies (*12, 13*), both D380A- and I477S- mutant myocilin secretion could be rescued by low-temperature culture, whereas little or no secretion could be rescued with I477N or K423E mutant myocilin. The latter two mutants are also observed as aggregates in the ER and induce the unfolded protein response (*10, 19*) (summarized in Table 1).

Expression and purification of MBP-OLF mutants followed closely procedures used for MBP-OLF(wt) (Figure 1, panel c), with similar yields (~1 mg purified mutant protein/ L culture). Experiments with mutants were conducted within a few days of purification. Like MBP-OLF(wt), three species were isolated by SEC, but based on peak height, the amount of aggregate mutant MBP-OLF in the void volume relative to that of isolated in a monomeric form, varied from ~1.8 ± 0.4 for MBP-OLF(wt), 3.4 ± 0.2 for the D380A OLF domain mutant (MBP-OLF(D380A)), 12.1 ± 2.1 for the I477N (MBP-OLF(I477N)), 14.2 ± 2.0 I477S for the mutant MBP-OLF(I477S), and 33.4 ± 3.6 for the K423E OLF domain mutant (MBP-OLF(K423E)). These ratios were unaffected by protein handling or concentration. Prolonged incubation at 4 °C leads to degradation of the OLF domain, as observed by SDS-PAGE (not shown); interconversion between aggregates and monomer is not seen (Supplementary Figure S1). Thus, OLF appears to harbor inherent aggregation propensity, in spite of cytosolic isolation from *E. coli*. After 37 °C incubation with Factor Xa, OLF is degraded, and cleavage could not be optimized to isolate the mutant OLF. However, at RT, circular dichroism (CD) spectra of the monomeric MBP-OLF mutants exhibit a mixture of the predominantly α-helical MBP (minima at 208, 222 nm) and predominantly β-sheet OLF (*23*) (minimum at 217 nm), with some variation in overall intensity indicative of primarily local changes in structure (Supplementary Figure S2). The disulfide bond remains intact in all of these mutants (Supplementary Table S1).

Thermal Stability Assay. The ability to express and purify site-directed MBP-OLF mutants in *E. coli* similar to MBP-OLF(wt), combined with similar CD signatures and disulfide bond retention, suggests that these mutants are folded and retain a native-like structure at or below RT. Thus, we developed a stability assay to compare wt OLF with that of mutants using a method that could be modified to test many mutants and stabilizing compounds.

We adapted the fluorescence thermal shift assay described originally for screening buffer conditions and stabilizing compounds (*34*) to compare wt to mutant MBP-OLFs as fusion proteins. The assay uses a real time (RT)-PCR instrument to conduct a slow melt while measuring fluorescence. The excitation and emission settings of the RT-PCR instrument are compatible with Sypro Orange, a dye known to bind to hydrophobic regions of proteins, which becomes increasingly exposed as the temperature of the protein−dye solution is raised. The melting temperature (T_m) is the midpoint of the transition given the upper and lower limits of the fluorescence signal and assumes a two-state transition. Whereas other studies using fluorescence thermal shift assays have explored protein stability as a function of buffer or ligand (*35, 36*) or mutants of a small four-helix bundle (*37*), our study appears to be a novel application of the assay to an explicitly aggregation-prone domain with disease relevance.

The fluorescence assay provides a reproducible, precise (~ ± 1 °C; Table 2), and convenient way to measure relative protein stability. The assay was used first to evaluate the T_m of cleaved, wt MYOC-OLF, which exhibits a reproducible transition at 52.7 ± 0.3 °C at neutral pH (Figure 2, panel a). To expand to mutant MBP-OLF fusion proteins, which cannot be cleaved with Factor Xa, we examined next the thermal stability of MBP alone (Figure 2, panel b) and compared MBP-OLF(wt) and
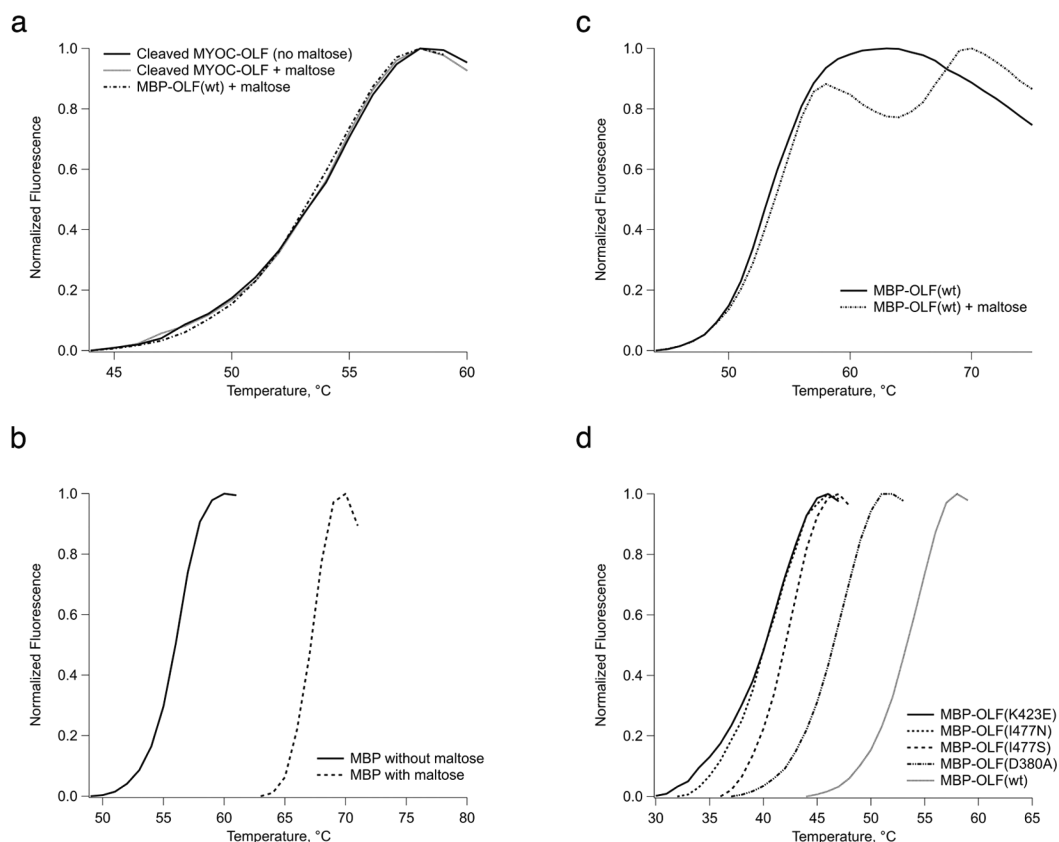
Figure 2. Melting curves. a) Cleaved MYOC-OLF with and without maltose. b) MBP melting with and without maltose. c) MBP-OLF with and without maltose. d) Comparison of mutant MBP-OLF stability.

cleaved OLF each with and without maltose (Figure 2 panels a and c). Apo MBP, which was isolated after Factor Xa cleavage of MBP-OLF(wt), exhibits a transition at 56.1 °C, and the addition of excess maltose shifts the T_m to 67.1 °C. These values are somewhat lower than those obtained for MBP from *E. coli* K-12 by differential scanning calorimetry (~64 °C without and ~72 °C with maltose at neutral pH) (*38, 39*), but two amino acid sequence differences and the C-terminal linker may contribute to this discrepancy. MBP-OLF(wt) without maltose exhibits a broad transition with a T_m of 51.8 °C. With maltose, two discrete transitions are observed for MBP-OLF(wt), one at 52.7 °C and the other at ~67 °C. The former overlaps well with cleaved OLF (Figure 2, panel a) and indicates that the first transition in the MBP-OLF fusion protein corresponds to the OLF domain. Compared to results with MBP, the second transition in MBP-OLF with maltose present is likely maltose-bound

MBP. The T_m of cleaved MYOC-OLF is not affected by the presence of maltose (Figure 2, panel a). These experiments establish that in the presence of maltose at pH 7, the T_m of the OLF domain is not affected by the presence of either MBP or maltose.

In comparison to MBP-OLF(wt), all four MBP-OLF mutants tested were destabilized but retained a discrete melting transition expected for a folded protein (Figure 2, panel d, Table 2). The transitions for MBP overlap well (not shown), reinforcing the independence of the two domains in the assay. MBP-OLF(D380A), associated with a mild glaucoma phenotype, exhibited the highest T_m (46.1 °C). This result is consistent with the observation that MBP-OLF(D380A) was expressed and purified in the highest yield among the mutants, and in cell studies is partially secreted at 37 °C (*12*) and largely secreted at 30 °C (*12, 13*). MBP-OLF(I477S), associated with a moderate myocilin glaucoma phenotype, showed

the next highest T_m of 41.9 °C, while the remaining two mutant proteins exhibit similar T_m's to each other, near 40 °C. Given that the temperature of the anterior eye is ~35 °C (40), a significant population of unfolded, aggregation prone mutant OLF domain is expected to be present. MBP-OLF(K423E) exhibits a weak pretransition prior to the major unfolding transition, which may have origins in extra instability conferred by charge inversion at this location in the OLF domain. The trend in T_m appears to follow generally the severity of aggregation and disease, although a strong correlation with disease phenotype will require the assessment of the stability of numerous other disease-causing MYOC-OLF mutants.

Stabilization of MBP-OLFs with Osmolytes. A shift of the population to a more stable, native-like myocilin could be an effective therapeutic intervention for myocilin glaucoma that could be delivered topically to the eye. Compounds could include those with general stabilizing ability called chemical chaperones or those tailored to bind a particular target, called pharmacological chaperones. There are several ways that a chaperone may help trafficked proteins, both wt and mutant, meet the ER quality control requirements, which include both thermodynamic- and kinetics-based mechanisms. For example, the chaperone could (i) accelerate folding, reducing the chance that it will be recognized as unfolded; (ii) bind and stabilize a fully folded protein so that it is less likely to unfold or to be recognized as misfolded; (iii) stabilize the protein for post-translational modification or interaction with a binding partner required for proper trafficking; or (iv) all or some combination of the above.

Numerous studies on potential pharmacological chaperones are focused on thermodynamic stabilization (20, 40–43). Even in the case of transthyretin, in which chaperones decrease the rate of amyloid fibril formation, the tetrameric state of protein is stabilized (44). Thus, drawing upon these examples, we believe that an important feature of a therapeutic compound for myocilin glaucoma will be restoration of myocilin stability to near wt levels. We further suggest that therapeutic agents should enable mutant myocilin to pass ER quality control, be secreted from HTM cells, and prevent myocilin from aggregating in the TEM. The latter effect could also include promoting proper interactions that maintain TEM integrity.

As proof-of-principle that mutant myocilins can be stabilized, we selected a subset of chemical chaper-

ones called osmolytes, low molecular weight agents that improve protein homeostasis in eukaryotic cells in response to osmotic stress (45). Osmolytes stabilize proteins not by direct ligand interaction but by destabilizing the unfolded state of the protein relative to that of the native, an effect thought to be due largely to unfavorable interactions of the protein backbone with the osmolyte-rich environment (46–49). In this study, we examined the effects of betaine, glycerol, proline, sarcosine, sucrose, trimethylamine N-oxide (TMAO), and 4-phenylbutyrate (4-PBA) on MYOC-OLF and MBP-OLF mutants (Figure 3). The last compound, 4-PBA, is not explicitly an osmolyte but is a chemical chaperone originally identified for treatment of urea cycle disorders. Although these compounds do not necessarily bind to MYOC-OLF as ligands, any that are found to stabilize myocilin are in principle of therapeutic potential and are, therefore, good test cases for evaluating the effects of small molecules on myocilin using the fluorescence stability assay.

First, we compared the effects of these chemical chaperones on MBP alone, MBP-OLF(wt), and MYOC-OLF, at several concentrations. As expected, there is a concentration dependence of the chaperone on the extent of stabilization. We focused on a concentration of 3 M chaperone, except for 4-PBA and TMAO where indicated, based on previous *in vitro* studies (50–53), ease of preparing solutions, and significant stability enhancement observed (Table 2, Figure 3). Comparison of MBP-OLF(wt) and cleaved MYOC-OLF reveals only a small difference (~0.3 °C) in T_m for all compounds tested (not shown). For this reason, we report in Table 2 only the results for MBP-OLF and for corresponding mutants. In addition, compared to MBP-OLF, the extent of MBP stabilization is generally a lower magnitude (Table 2). Thus, the comparison of mutant MBP-OLF stability reflects the effect on the MYOC-OLF domain alone.

The chaperone effects on MYOC-OLF(wt) rank as follows: sarcosine ~ TMAO ~ sucrose (8−10 °C) ≫ proline ~ betaine ~ glycerol (2−4 °C) > 4-PBA (~0 °C) (Table 2, Figure 3). Given that osmolytes confer only limited stability to proteins *via* side chain effects (46), the degree of stabilization of the mutants should be relatively consistent with that of MYOC-OLF(wt). Notably, sarcosine is structurally similar to the less effective betaine, illustrating the complexity of protein stabilization by osmolytes.
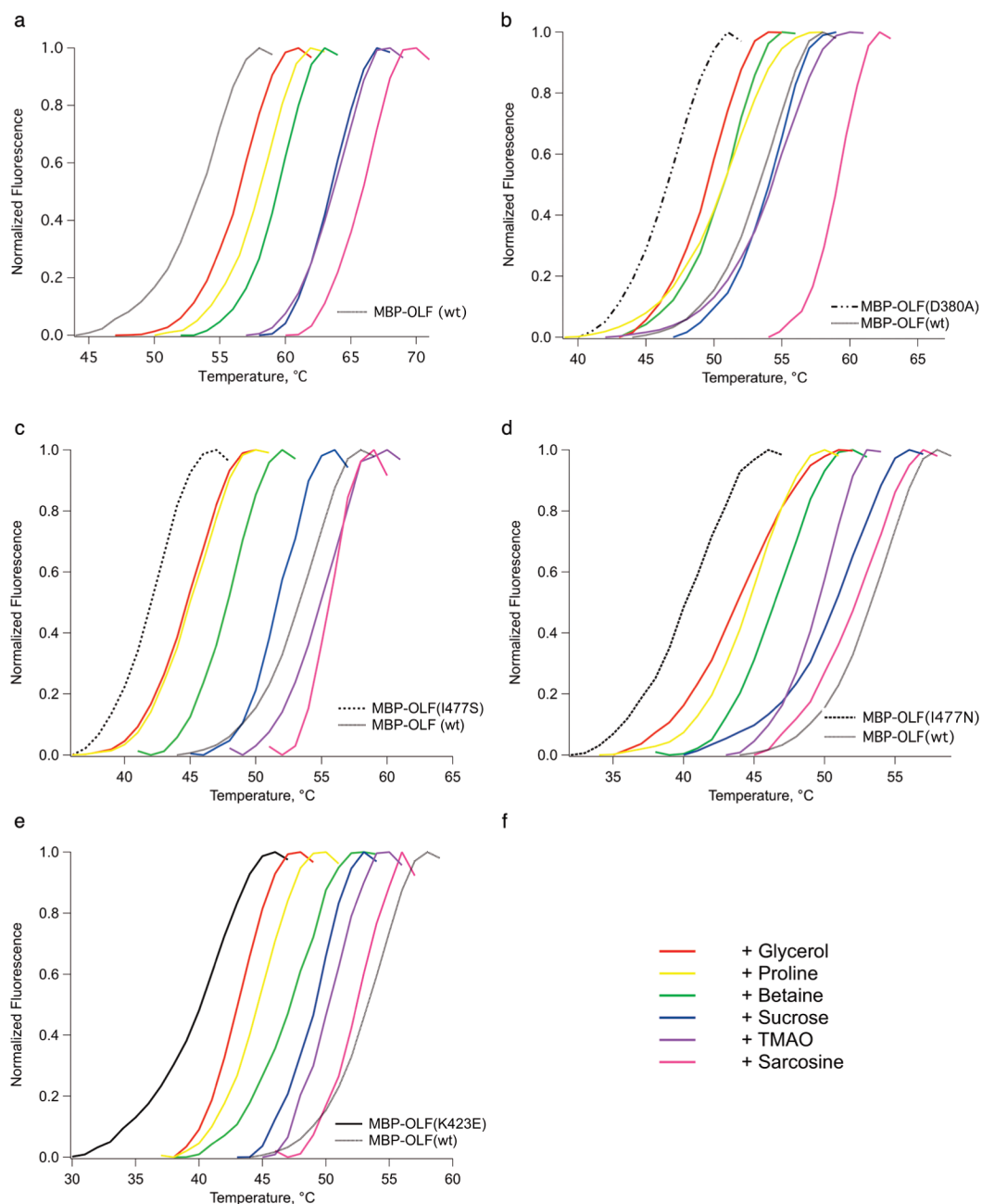
BURNS *ET AL.*

Figure 3. Effects of osmolytes on MBP-OLF stability. a) MBP-OLF(wt). b) MBP-OLF(D380A). c) MBP-OLF(I477S). d) MBP-OLF(I477N). e) MBP-OLF(K423E). For panels b–e, MBP-OLF mutant (no osmolyte) appears as the leftmost melting curve using the same scheme as in Figure 2, panel d, and MBP-OLF(wt) appears as gray. f) Color key to osmolytes.

Sarcosine, TMAO, and, to a lesser extent, sucrose, were effective at 3 M in improving mutant MBP-OLF stability. For MBP-OLF(D380A), better than wt stability

(Figure 3, panel b) was achieved for all three osmolytes, a result that is not surprising given that the ΔT_m between MBP-OLF(wt) and MBP-OLF(D380A) is smaller

than the ΔT_m of MBP-OLF(wt) with the same osmolytes (Table 2). For both I477 variants (Figure 3, panels c and d), sarcosine gave the highest ΔT_m; the OLF domain is stabilized to the same degree when substituted with either the small Ser or the similar-sized Asn side chains. By contrast, MBP-OLF(K423E) (Figure 3, panel e) is relatively resistant to stabilization by chemical chaperones. For each, the extent of stabilization of MBP-OLF(K423E) was less than for the wt and the other three mutants. Even in the presence of 5 M TMAO, the T_m could only be increased to a value between wt and MBP-OLF(D380A) without osmolytes (Table 2). Moreover, transitions observed for MBP-OLF(K423E) with TMAO and sarcosine, while shifted considerably, were correlated with more modest changes in the Sypro Orange fluorescence signal in the assay. The effects of the strongly stabilizing osmolytes on MBP-OLF variants observed here are consistent with evidence for more compact protein structures in osmolyte solutions (54), which is expected to be most challenging to accomplish for the charge inversion in MBP-OLF(K423E).

Compared to the transitions observed for osmolyte-stabilized MBP-OLF(wt), all of which appear to have the same shape, those of the corresponding melting curves for mutants differ. A shallow pretransition is observed for MBP-OLF(D380A) with proline and TMAO, whereas the remaining osmolytes follow closely the shape of the curve in the absence of osmolyte (Figure 3, panel b). Pretransitions are also apparent for MBP-OLF(I477N) with glycerol and sucrose (Figure 3, panel d). Conversely, sharper transitions are seen for MBP-OLF(I477S) in the presence of sarcosine compared to that of other osmolytes. These comparisons suggest a deviation from the assumed two-state behavior of a single domain unfolding. An intermediate species enabled by non-native interactions may exist in mutant myocilins prior to full denaturation. In sum, the effects of osmolytes, which are generally believed to be an effect due to interactions with the protein backbone, may also be influenced by the side chains in terms of either an unfolding pathway or an unfavorable side chain environment, such as charge inversion, that limit the extent of stability achievable.

Our stabilization results differ from previous cellular trafficking studies using green fluorescence protein (GFP)-tagged mutant myocilin (C245Y, G364V, P370L, Y347H) (28) or FLAG-tagged mutant myocilin (D380N) (55). These studies monitored myocilin secretion at a single concentration (mM) of glycerol (28), 4-PBA (28), or TMAO (28) by immunoprecipitation/Western blot of myocilin in the media, in combination with immunofluorescence to detect myocilin retained in the ER. Chaperones 4-PBA and TMAO showed a two-fold increase in secretion. Chemical chaperones act nonspecifically, so cellular studies do not establish a direct stabilizing effect on myocilin. Whereas no effect on secretion was seen with glycerol in cell studies (28), we found a modest increase in mutant OLF stability, albeit at much higher concentrations not tested in cells. In addition, in contrast to the rescue of secretion observed with 4-PBA, this compound had no direct stabilizing effect on wt MYOC-OLF in vitro at low mM concentrations and was strongly destabilizing above 10 mM (not shown). Only TMAO appears to both stabilize in vitro and promote secretion from HTM cells, although the effects were observed with different mutants. These limited comparisons stress the need for complementary studies to evaluate molecules that stabilize mutant myocilins directly and promote its secretion in cells, both of which are key to developing a new treatment for myocilin glaucoma.

METHODS

Molecular Biology. The MYOC-OLF gene was amplified (using 5-PRIME MasterMix) from a plasmid reported previously (56), annealed into the pET-30 Xa/LIC vector (Novagen), and then subcloned into the pMAL-c4x vector. The final pMAL-c4x construct incorporates an eight amino acid linker between MBP and OLF (SSSEIGR), where the Factor Xa cleavage sequence is leftover from pET-30 Xa/LIC. After plasmid replication in NovaBlue Gigasingles (Novagen), the plasmid was isolated (QIAPrep, Qiagen). Mutant MBP-OLFs were generated by the site-directed mutagenesis (QuikChange, Stratagene) kit. Primers are listed in Table 3. All plasmids were verified by DNA sequencing (Operon).

Protein Expression and Purification. Wild-type and mutant plasmids were transformed into Rosetta-gami 2(DE3)pLysS (Novagen) cells and cultured in Superior Broth (US Biological) to an optical density of ~0.7 at 600 nm, cooled to 18 °C, and induced with 0.5 mM isopropyl β-D-thiogalactopyranoside (IPTG). After overnight growth (12−16 h), cells were pelleted, flash frozen, and stored at −80 °C.

Cell pellets were lysed by French Press in the presence of 50 mM HEPES pH = 7.5, 200 mM NaCl, 1 mM EDTA (buffer A), and supplemented with Roche Complete Protease Inhibitor Cocktail tablets. Cell debris was removed by centrifugation (5000 g for 15 min), and supernatant was loaded onto a 20 mL high-flow amylose resin (New England Biolabs) column equili-

TABLE 3. Primers used in this study

Plasmid template	Target vector		Primer used
		MYOC-OLF cloning	
pcDNA	pET-30XaLIC	Forward	5'-GGTATTGAGGGTCGCTTGAAGGAGAGCCCATCTG
		Reverse	5'-AGAGGAGAGTTAGAGCCTTATCACATCTTGGAGAGCTTGATG
pET-30XaLIC	pMAL-c4x	Forward	5'-CGCCGAGCTCTATTGAGGGTCGC
		Reverse	5'-GCCGAATTCAGGAGAGTTAGAGCCTTATCA
		Mutagenesis	
D380A			5'-GCTACACGGACATTGCCTTGGCTGTGGATG
K423E			5'-GGGAGACAAACATCCGTGAACAGTCAGTCGCCAATGCC
I477N			5'-GTACAGCAGCATGAATGACTACAACCCCCTGG
I477S			5'-GTACAGCAGCATGTCTGACTACAACCCCCTCG

brated with buffer A. The MBP-OLFs were eluted with buffer A plus 10 mM maltose, concentrated using an Amicon Ultra YM-10 centrifugation device, and either flash frozen and stored at −80 °C or loaded on a gel filtration on a Superdex 75 prep-grade column (GE Healthcare) equilibrated with 10 mM Phosphate (Na/K), 200 mM NaCl, and pH = 7.2 (buffer B). Only those fractions corresponding to monomeric MBP-OLF were pooled for further use.

Cleavage of MBP-OLF(wt) was accomplished by overnight (~16 h) incubation with Factor Xa (New England Biolabs) in 50 mM Tris pH = 8, 100 mM NaCl, and 5 mM CaCl$_2$. After capture of Factor Xa (Xarrest, Novagen), cleaved OLF was fractionated from uncleaved material and MBP by taking the flowthrough fraction from the amylose resin for purification on Superdex 75. MBP used in these studies was also isolated this way. Protein in the experiments was used within three days of purification. SDS-PAGE analysis was conducted as described (57).

Thermal Stability Assay. Sypro Orange (Invitrogen), supplied as a 5000 X solution in dimethylsulfoxide, was diluted in the buffer solution (1:1000) and mixed well just prior to preparing samples for the assay. Reactions of 30 μL were prepared at RT and delivered to 96-well optical plates (Applied Biosystems) before sealing with optical film. To the protein solutions at a final concentration of 0.5−1.5 μM in buffer B, 3 μL of diluted Sypro Orange were added. Except when indicated otherwise, maltose was present at 50 mM. Compounds tested for stability enhancement were obtained from commercial sources. Where indicated, TMAO and sarcosine were tested at 5 M in the reaction buffer, whereas 4-PBA was tested in a concentration range of 1 mM−0.5 M. For all others, a 5 M stock was diluted to 3 M in buffer B. Plates included a baseline control containing Sypro Orange with no protein. The pH of the final solutions did not deviate significantly from 7.

Fluorescence data were acquired on an Applied Biosciences Step-One Plus RT-PCR instrument equipped with a fixed excitation wavelength (480 nm) and a ROX emission filter (610 nm). Melts were conducted from 25−95 °C with a 1 °C per min increase. No difference in T_m was observed when the rate of heating was slowed to 0.5 °C per min. Above a minimum threshold of protein concentration required to observe a discrete transition, no dependence of protein concentration on T_m was observed. Data were processed using GraphPad Prism. After baseline subtraction, data were trimmed to include both the boundaries and the transition of interest and were normalized.

The reported T_m is the inflection point of the sigmoidal curve, which was fit as described previously (34).

Supporting Information Available: This material is available free of charge *via* the Internet.

REFERENCES

1. Kwon, Y. H., Fingert, J. H., Kuehn, M. H., and Alward, W. L. (2009) Primary open-angle glaucoma, *N. Engl. J. Med. 360*, 1113−1124.

2. Alward, W. L. (1998) Medical management of glaucoma, *N. Engl. J. Med. 339*, 1298−1307.

3. Resch, Z., and Fautsch, M. (2009) Glaucoma-associated myocilin: A better understanding but much more to learn, *Exp. Eye Res. 88*, 704−712.

4. Gasiorowski, J., and Russell, P. (2009) Biological properties of trabecular meshwork cells, *Exp. Eye Res. 88*, 671−675.

5. Wentz-Hunter, K., Kubota, R., Shen, X., and Yue, B. (2004) Extracellular myocilin affects activity of human trabecular meshwork cells, *J. Cell. Physiol. 200*, 45−52.

6. Goldwich, A., Scholz, M., and Tamm, E. R. (2009) Myocilin promotes substrate adhesion, spreading and formation of focal contacts in podocytes and mesangial cells, *Histochem. Cell Biol. 131*, 167−180.

7. Filla, M. S., Liu, X., Nguyen, T. D., Polansky, J. R., Brandt, C. R., Kaufman, P. L., and Peters, D. M. (2002) In vitro localization of TIGR/MYOC in trabecular meshwork extracellular matrix and binding to fibronectin, *Invest. Ophthalmol. Visual Sci. 43*, 151−161.

8. Fautsch, M. P., and Johnson, D. H. (2001) Characterization of myocilin-myocilin interactions, *Invest. Ophthalmol. Visual Sci. 42*, 2324−2331.

9. Tomarev, S. I., and Nakaya, N. (2009) Olfactomedin domain-containing proteins: possible mechanisms of action and functions in normal development and pathology, *Mol. Neurobiol. 40*, 122–138.

10. Joe, M. K., Sohn, S., Hur, W., Moon, Y., Choi, Y. R., and Kee, C. (2003) Accumulation of mutant myocilins in ER leads to ER stress and potential cytotoxicity in human trabecular meshwork cells, *Biochem. Biophys. Res. Commun. 312*, 592–600.

11. Liu, Y., and Vollrath, D. (2004) Reversal of mutant myocilin non-secretion and cell killing: implications for glaucoma, *Hum. Mol. Genet. 13*, 1193–1204.

12. Vollrath, D., and Liu, Y. (2006) Temperature sensitive secretion of mutant myocilins, *Exp. Eye Res. 82*, 1030–1036.

13. Gobeil, S., Letartre, L., and Raymond, V. (2006) Functional analysis of the glaucoma-causing TIGR/myocilin protein: integrity of amino-terminal coiled-coil regions and olfactomedin homology domain is essential for extracellular adhesion and secretion, *Exp. Eye Res. 82*, 1017–1029.

14. Kim, B. S., Savinova, O. V., Reedy, M. V., Martin, J., Lun, Y., Gan, L., Smith, R. S., Tomarev, S. I., John, S. W., and Johnson, R. L. (2001) Targeted disruption of the myocilin gene (Myoc) suggests that human claucoma-causing mutations are gain of function, *Mol. Cell. Biol. 21*, 7707–7713.

15. Lam, D. S., Leung, Y. F., Chua, J. K., Baum, L., Fan, D. S., Choy, K. W., and Pang, C. P. (2000) Truncations in the TIGR gene in individuals with and without primary open-angle glaucoma, *Invest. Ophthalmol. Visual Sci. 41*, 1386–1391.

16. Ellgaard, L., and Helenius, A. (2003) Quality control in the endoplasmic reticulum, *Nat. Rev. Mol. Cell. Biol. 4*, 181–191.

17. Yam, G. H.-F., Gaplovska-Kysela, K., Zuber, C., and Roth, J. (2007) Aggregated myocilin induces russell bodies and causes apoptosis: implications for the pathogenesis of myocilin-caused primary open-angle glaucoma, *Am. J. Pathol. 170*, 100–109.

18. Wang, L., Zhuo, Y., Liu, B., Huang, S., Hou, F., and Ge, J. (2007) Pro370Leu mutant myocilin disturbs the endoplasm reticulum stress response and mitochondrial membrane potential in human trabecular meshwork cells, *Mol. Vision 13*, 618–625.

19. Carbone, M. A., Ayroles, J. F., Yamamoto, A., Morozova, T. V., West, S. A., Magwire, M. M., Mackay, T. F. C., and Anholt, R. R. H. (2009) Overexpression of myocilin in the Drosophila eye activates the unfolded protein response: implications for glaucoma, *PLoS One 4*, e4216.

20. Powers, E. T., Morimoto, R. I., Dillin, A., Kelly, J. W., and Balch, W. E. (2009) Biological and chemical approaches to diseases of proteostasis deficiency, *Annu. Rev. Biochem. 78*, 959–991.

21. Cohen, F. E., and Kelly, J. W. (2003) Therapeutic approaches to protein-misfolding diseases, *Nature 426*, 905–909.

22. Fautsch, M. P., Vrabel, A. M., Peterson, S. L., and Johnson, D. H. (2004) In vitro and in vivo characterization of disulfide bond use in myocilin complex formation, *Mol. Vision 10*, 417–425.

23. Nagy, I., Trexler, M., and Patthy, L. (2003) Expression and characterization of the olfactomedin domain of human myocilin, *Biochem. Biophys. Res. Commun. 302*, 554–561.

24. Peters, D. M., Herbert, K., Biddick, B., and Peterson, J. A. (2005) Myocilin binding to Hep II domain of fibronectin inhibits cell spreading and incorporation of paxillin into focal adhesions, *Exp. Cell Res. 303*, 218–228.

25. Park, B. C., Shen, X., Fautsch, M. P., Tibudan, M., Johnson, D. H., and Yue, B. Y. (2006) Optimized bacterial expression of myocilin proteins and functional comparison of bacterial and eukaryotic myocilins, *Mol. Vision 12*, 832–840.

26. Eswari Pandaranayaka, P. J., Kanagavalli, J., Krishnadas, S. R., Sundaresan, P., and Krishnaswamy, S. (2008) Over expression and purification of recombinant human myocilin, *World J. Microbiol. Biotechnol. 24*, 903–907.

27. di Guan, C., Li, P., Riggs, P. D., and Inouye, H. (1988) Vectors that facilitate the expression and purification of foreign peptides in Escherichia coli by fusion to maltose-binding protein, *Gene 67*, 21–30.

28. Yam, G. H.-F., Gaplovska-Kysela, K., Zuber, C., and Roth, J. (2007) Sodium 4-phenylbutyrate acts as a chemical chaperone on misfolded myocilin to rescue cells from endoplasmic reticulum stress and apoptosis, *Invest. Ophthalmol. Visual Sci. 48*, 1683–1690.

29. Trovato, A., Seno, F., and Tosatto, S. C. (2007) The PASTA server for protein aggregation prediction, *Protein Eng., Des. Sel. 20*, 521–523.

30. Kennan, A. M., Mansergh, F. C., Fingert, J. H., Clark, T., Ayuso, C., Kenna, P. F., Humphries, P., and Farrar, G. J. (1998) A novel Asp380Ala mutation in the GLC1A/myocilin gene in a family with juvenile onset primary open angle glaucoma, *J. Med. Genet. 35*, 957–960.

31. Stoilova, D., Child, A., Brice, G., Desai, T., Barsoum-Homsy, M., Ozdemir, N., Chevrette, L., Adam, M. F., Garchon, H. J., Pitts Crick, R., and Sarfarazi, M. (1998) Novel TIGR/MYOC mutations in families with juvenile onset primary open angle glaucoma, *J. Med. Genet. 35*, 989–992.

32. Richards, J. E., Ritch, R., Lichter, P. R., Rozsa, F. W., Stringham, H. M., Caronia, R. M., Johnson, D., Abundo, G. P., Willcockson, J., Downs, C. A., Thompson, D. A., Musarella, M. A., Gupta, N., Othman, M. I., Torrez, D. M., Herman, S. B., Wong, D. J., Higashi, M., and Boehnke, M. (1998) Novel trabecular meshwork inducible glucocorticoid response mutation in an eight-generation juvenile-onset primary open-angle glaucoma pedigree, *Ophthalmology 105*, 1698–1707.

33. Morissette, J., Cote, G., Anctil, J. L., Plante, M., Amyot, M., Heon, E., Trope, G. E., Weissenbach, J., and Raymond, V. (1995) A common gene for juvenile and adult-onset primary open-angle glaucomas confined on chromosome 1q, *Am. J. Hum. Genet. 56*, 1431–1442.

34. Niesen, F. H., Berglund, H., and Vedadi, M. (2007) The use of differential scanning fluorimetry to detect ligand interactions that promote protein stability, *Nat. Protoc. 2*, 2212–2221.

35. Vedadi, M., Niesen, F. H., Allali-Hassani, A., Fedorov, O. Y., Finerty, P. J., Jr., Wasney, G. A., Yeung, R., Arrowsmith, C., Ball, L. J., Berglund, H., Hui, R., Marsden, B. D., Nordlund, P., Sundstrom, M., Weigelt, J., and Edwards, A. M. (2006) Chemical screening methods to identify ligands that promote protein stability, protein crystallization, and structure determination, *Proc. Natl. Acad. Sci. U.S.A. 103*, 15835–15840.

36. Giuliani, S. E., Frank, A. M., and Collart, F. R. (2008) Functional assignment of solute-binding proteins of ABC transporters using a fluorescence-based thermal shift assay, *Biochemistry 47*, 13974–13984.

37. Lavinder, J. J., Hari, S. B., Sullivan, B. J., and Magliery, T. J. (2009) High-throughput thermal scanning: a general, rapid dye-binding thermal shift screen for protein engineering, *J. Am. Chem. Soc. 131*, 3794–3795.

38. Novokhatny, V., and Ingham, K. (1997) Thermodynamics of maltose binding protein unfolding, *Protein Sci. 6*, 141–146.

39. Ganesh, C., Shah, A. N., Swaminathan, C. P., Surolia, A., and Varadarajan, R. (1997) Thermodynamic characterization of the reversible, two-state unfolding of maltose binding protein, a large two-domain protein, *Biochemistry 36*, 5020–5028.

40. Rosenbluth, R. F., and Fatt, I. (1977) Temperature measurements in the eye, *Exp. Eye Res. 25*, 325–341.

41. Lieberman, R. L., D'aquino, J. A., Ringe, D., and Petsko, G. A. (2009) Effects of pH and Iminosugar Pharmacological Chaperones on Lysosomal Glycosidase Structure and Stability, *Biochemistry 48*, 4816–4827.

42. Sawkar, A. R., Schmitz, M., Zimmer, K. P., Reczek, D., Edmunds, T., Balch, W. E., and Kelly, J. W. (2006) Chemical chaperones and permissive temperatures alter localization of Gaucher disease associated glucocerebrosidase variants, *ACS Chem. Biol. 1*, 235–251.

43. Loo, T. W., Bartlett, M. C., and Clarke, D. M. (2008) Correctors promote folding of the CFTR in the endoplasmic reticulum, *Biochem. J. 413*, 29–36.

44. Johnson, S. M., Wiseman, R. L., Sekijima, Y., Green, N. S., Adamski-Werner, S. L., and Kelly, J. W. (2005) Native state kinetic stabilization as a strategy to ameliorate protein misfolding diseases: a focus on the transthyretin amyloidoses, *Acc. Chem. Res. 38*, 911–921.

45. Balch, W. E., Morimoto, R. I., Dillin, A., and Kelly, J. W. (2008) Adapting Proteostasis for Disease Intervention, *Science 319*, 916–919.

46. Bolen, D. W., and Rose, G. D. (2008) Structure and energetics of the hydrogen-bonded backbone in protein folding, *Annu. Rev. Biochem. 77*, 339–362.

47. Bolen, D. W., and Baskakov, I. V. (2001) The osmophobic effect: natural selection of a thermodynamic force in protein folding1, *J. Mol. Biol. 310*, 955–963.

48. Arakawa, T., and Timasheff, S. N. (2005) The stabilization of proteins by osmolytes, *Biophys. J. 47*, 411–414.

49. Arakawa, T., Ejima, D., Kita, Y., and Tsumoto, K. (2006) Small molecule pharmacological chaperones: From thermodynamic stabilization to pharmaceutical drugs, *Biochem. Biophys. Acta. 1746*, 1677–1687.

50. Wang, A., Robertson, A. D., and Bolen, D. W. (1995) Effects of a naturally occurring compatible osmolyte on the internal dynamics of ribonuclease A, *Biochemistry 34*, 15096–15104.

51. Wang, A., and Bolen, D. W. (1997) A naturally occurring protective system in urea-rich cells: mechanism of osmolyte protection of proteins against urea denaturation, *Biochemistry 36*, 9101–9108.

52. Liu, Y., and Bolen, D. W. (1995) The peptide backbone plays a dominant role in protein stabilization by naturally occurring osmolytes, *Biochemistry 34*, 12884–12891.

53. Wu, P., and Bolen, D. W. (2006) Osmolyte-induced protein folding free energy changes, *Proteins 63*, 290–296.

54. Street, T. O., Krukenberg, K. A., Rosgen, J., Bolen, D. W., and Agard, D. A. (2010) Osmolyte-induced conformational changes in the Hsp90 molecular chaperone, *Protein Sci. 19*, 57–65.

55. Jia, L.-Y., Gong, B., Pang, C.-P., Huang, Y., Lam, D. S.-C., Wang, N., and Yam, G. H.-F. (2009) Correction of the disease phenotype of myocilin-causing glaucoma by a natural osmolyte, *Invest. Ophthalmol. Visual Sci. 50*, 3743–3749.

56. Zhou, Z., and Vollrath, D. (1999) A cellular assay distinguishes normal and mutant TIGR/myocilin protein, *Hum. Mol. Genet. 8*, 2221–2228.

57. Sambrook, J., Russell, D. W. (2001) *Molecular cloning: a laboratory manual*, 3rd ed., Cold Spring Harbor Laboratory Press, Cold Spring Harbor, N.Y.